The atomic structure and chemistry of Fe-rich steps on antiphase boundaries in Ti-doped Bi0.9Nd0.15FeO3

Ian MacLaren, LiQiu Wang, Alan J. Craven, Quentin M. Ramasse, Bernhard Schaffer, Kambiz Kalantari, and Ian M. Reaney

Citation: APL Materials **2**, 066106 (2014); doi: 10.1063/1.4884684
View online: http://dx.doi.org/10.1063/1.4884684
View Table of Contents: http://scitation.aip.org/content/aip/journal/aplmater/2/6?ver=pdfcov
Published by the AIP Publishing

APL MATERIALS **2**, 066106 (2014)

The atomic structure and chemistry of Fe-rich steps on antiphase boundaries in Ti-doped $Bi_{0.9}Nd_{0.15}FeO_3$

Ian MacLaren,[1,2,a] LiQiu Wang,[1] Alan J. Craven,[1,2] Quentin M. Ramasse,[2] Bernhard Schaffer,[1,2] Kambiz Kalantari,[3] and Ian M. Reaney[3]
[1]*SUPA School of Physics and Astronomy, University of Glasgow, Glasgow G12 8QQ, United Kingdom*
[2]*SuperSTEM Laboratory, SciTech Daresbury, Keckwick Lane, Warrington WA4 4AD, United Kingdom*
[3]*Department of Materials Science and Engineering, University of Sheffield, Mappin St, Sheffield S1 3JD, United Kingdom*

(Received 2 May 2014; accepted 10 June 2014; published online 23 June 2014)

Stepped antiphase boundaries are frequently observed in Ti-doped $Bi_{0.85}Nd_{0.15}FeO_3$, related to the novel planar antiphase boundaries reported recently. The atomic structure and chemistry of these steps are determined by a combination of high angle annular dark field and bright field scanning transmission electron microscopy imaging, together with electron energy loss spectroscopy. The core of these steps is found to consist of 4 edge-sharing FeO_6 octahedra. The structure is confirmed by image simulations using a frozen phonon multislice approach. The steps are also found to be negatively charged and, like the planar boundaries studied previously, result in polarisation of the surrounding perovskite matrix. [http://dx.doi.org/10.1063/1.4884684]

It has been previously shown that Ti-doping in $Bi_{0.9}Nd_{0.15}FeO_3$ suppresses conductivity via a donor doping mechanism and allows the ferroelectric and antiferroelectric phase transitions to be directly observed in temperature dependent dielectric data.[1] Ti-doping also modifies the Neel (T_N) and Curie (T_C) temperatures with T_N showing a linear decrease but T_C a non-linear dependence.[1] Whilst much of the Ti doping enters the perovskite structure as a randomly distributed B-site dopant, uncompensated Ti doping on the B-site causes precipitation of NdO_x nanorods, with a novel core-structure just two atoms across.[2] The nanorods are present due to the ex-solution of Nd ions[3] and are accompanied by the formation of vacancies ($V_{Nd}^{///}$) in the perovskite matrix that compensate for the Ti substitution onto Fe sites ($Fe_{Ti}^{\bullet}$).

Additionally, Ti doping causes the formation of unique antiphase boundaries (APBs), never previously seen in perovskites. These APBs have a core held together with edge-sharing octahedra, one of which is always a TiO_6 octahedron. Their chemical structure was reconstructed at 10 pm precision in 3 dimensions and it was shown that the core had excess negative charge which resulted in a strong polarisation of the surrounding perovskite and the stabilisation of a polar phase a few unit cells each side of the APB.[4] In this previous study, however, we restricted the discussion to planar sections of the boundaries on the (001) plane. In the present work, we show that such antiphase boundaries can deviate strongly from the {001} planes through the formation of stepped structures. We determine quantitatively the structure and chemistry of the steps, and propose a three-dimensional model consistent with the already known terrace structure.[4]

Atomic resolution high angle annular dark field (HAADF) images of a novel type of APB, taken from different areas by aberration corrected scanning transmission electron microscopy (STEM), are shown in Fig. 1. Such boundaries were frequently observed throughout this ceramic. In

[a]Author to whom correspondence should be addressed. Electronic mail: ian.maclaren@glasgow.ac.uk

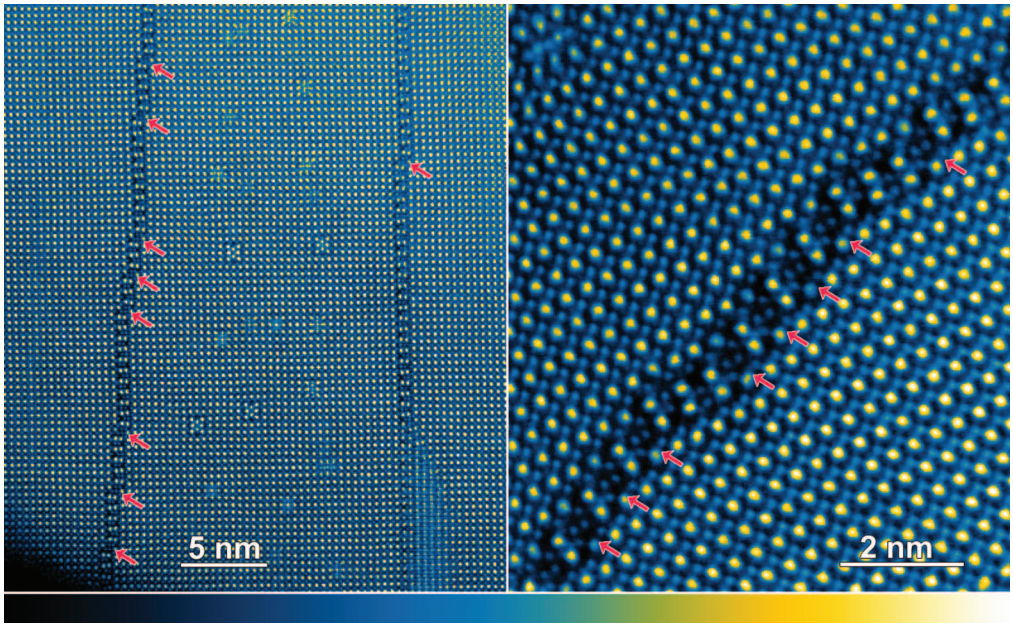

FIG. 1. Two examples of stepped structures on antiphase boundaries. In both cases, these are high angle annular dark field (HAADF) images and are represented on the false colour intensity scale shown below the images, the brighter atoms are the heavy A-site atoms (Bi/Nd), whereas the less bright atoms are the B-site atoms (Fe/Ti); O atoms are not visible in these images. The image to the left shows two parallel boundaries, one almost flat whilst the other is more stepped. Some nanorods are also observed between the boundaries. The image to the right shows a heavily stepped boundary, with very few flat terraces. The arrangement of B-site (Fe or Ti) columns in the steps is clearly shown in this image. The steps are indicated by pink arrows in the images.

Fig. 1(a), the central region between the two boundaries with nanorods viewed end-on[2] defines the [001] direction of the orthorhombic $PbZrO_3$-like structure.[1] The precise orientation of the orthorhombic axes in the regions to the left and the right of the APBs is undetermined. However, their difference in orientation with the [001] direction of the central region indicates that they are also twin domain boundaries. Such boundaries may be viewed as if they are constructed from two main structural units – flat terraces, as reported previously,[4] and steps, which are marked by arrows. Clearly from these images, steps appear adjacent or separated by terraces of varied length. Within the terraced part of the boundary, the key features are the vertical shift of one half of a primitive perovskite unit cell across the boundary, as required for an antiphase boundary, and the "ladder-like" appearance of pairs of brighter atom columns corresponding to the heavy Bi (A-site) atoms in the boundary alternating with pairs of weaker columns corresponding to the lighter Fe/Ti (B-site) atoms along the vertical direction. It should be noted that boundaries frequently have planar sections on ⟨100⟩ planes as reported previously,[4] as well as curved or inclined sections, with the curvature provided by these steps. These boundaries, stepped or planar are mainly terminated by interaction with internal grain boundaries in the ceramic, but have occasionally been observed to interact with each other.

To study the structure of the steps in more detail, the reader is directed to Figure 2, which shows a pair of HAADF and bright field (BF) images of one step (together with simulations which will be discussed later). The main feature of the core is four B-site atom columns and no A site columns. In fact, the step has a structure very similar to the ends of two terraces placed adjacent to one another, with a shift of one unit cell downwards, and any deviations from such a structure are minor. As in our previous studies using aberration-corrected STEM of the atomic structure of defects and nanostructures in oxides,[2,4,5] the positions of all atoms were quantified using the iMtools plugin, the resulting dataset processed to remove any linear scan distortions, and an atomic model constructed. In contrast to our prior work, it was impossible to use a second orthogonal projection to reveal the three dimensional positions of the atoms. However, a plausible three-dimensional model

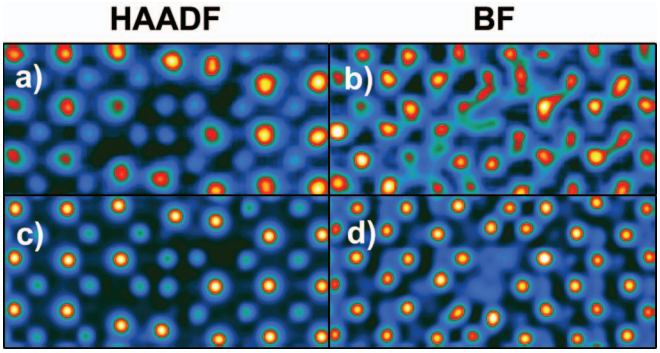

FIG. 2. Comparison of experimental and simulated HAADF and BF images of a step: (a) Experimental HAADF image; (b) experimental BF image recorded simultaneously; (c) simulated HAADF image; (d) simulated BF image.

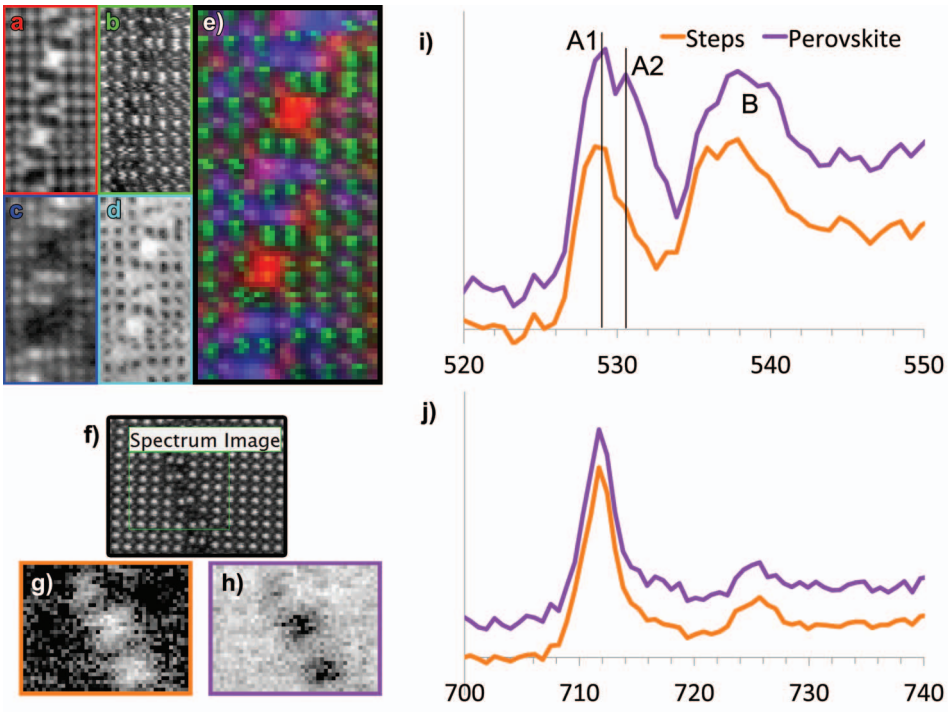

FIG. 3. Electron energy loss spectroscopy and spectrum imaging of the steps. (a)–(e) Chemical mapping of an area of antiphase boundary containing two steps: (a) Fe map, (b) HAADF signal (A-site atoms, i.e., Bi/Nd), (c) Ti map, (d) O map, and (e) RGB combined map of Fe, A-sites, and Ti. (f)–(j) ELNES mapping of an area with two steps: (f) the survey area, (g) MLLS fit map for the O ELNES from the step, (h) MLLS fit map for the O ELNES from the perovskite, (i) O-K ELNES comparison, and (j) Fe-$L_{2,3}$ ELNES comparison. Maps are formed after noise reduction of the datasets by PCA and smoothed by the application of a low pass filter.

could still be constructed using prior knowledge of the 3D structure of the terraces and sensible bonding criteria.

Figs. 3(a)–3(e) show elemental maps of two steps separated by a terrace of only one unit length, together with simultaneously recorded HAADF images to show the heavy A-site atom positions in the Red-Green-Blue (RGB) image of Figure 3(e). The strong Ti segregation to the terraces is consistent with results reported previously.[4] The notable feature of the steps, however, is that they contain almost no Ti whilst being rich in Fe and O. This indicates that the pairs of B-site atoms in steps are very different from the pairs of B-sites atoms in terraces, even if the interatomic distances are similar.

To further investigate the detailed chemical environment of the steps we looked in detail at the Electron Energy Loss Near Edges Structure (ELNES). Pairs of background-subtracted reference spectra were extracted from one Electron Energy Loss Spectroscopy (EELS) spectrum image, one for the perovskite matrix, and one for the step core; these pairs of reference spectra are displayed in Figure 3(i) for the O-K edge and Fig. 3(j) for the Fe-$L_{2,3}$ edge. The spectrum image was then fitted as a linear combination of these two spectra using the multiple linear least squares (MLLS) fitting technique (as implemented in Gatan Digital Micrograph). As the ELNES of the oxygen K-edge is well known to be highly sensitive to the nature of the 3*d* and other orbitals of the transition-metal oxides,[6–8] the oxygen K-edge spectra from the perovskite and steps shown in Fig. 3(i) were chosen as the reference spectra for the mapping. Figs. 3(g) and 3(h) show the fit-coefficient maps corresponding to these two reference spectra. The O K-edge ELNES shown here in Figure 3(i) from the perovskite is in good agreement with theoretical calculations and previous experimental reports[8,9] with a clear splitting of the first A peak into two subpeaks, A1 and A2, the latter of which was attributed by Saeterli *et al.*[9] to the combined influence of backscattering on O^{2-} ions together with hybridisation of O 2*p* states with *p*-like states in Bi. Additionally, Saeterli *et al.*[9] found that in $Bi_{0.9}La_{0.1}FeO_3$ that the substitution of the rare earth ion for Bi also weakened the A peak but increased slightly the A2/A1 intensity ratio and that there were some contributions from the rare earth ion to the A2 peak; similar effects would be expected for Nd substitution, as in the present work. It is therefore natural to expect that this A2 peak may be depressed in the absence of Bi and Nd, as in the steps in our work. It is therefore not surprising that the O-K ELNES from the step is significantly different to that from the perovskite and is closer to reported spectra from iron oxides. On comparison with spectra of α/γ-Fe_2O_3 reported by Paterson *et al.*,[10] the step displays an O-K ELNES more similar to γ-Fe_2O_3, specifically in the shape of the A peak, which mainly peaks at the A1 position and displays little intensity at the A2 position.

The B peak further behind the edge (around 538eV) also changes shape between the perovskite and the step regions, and peaks earlier and finishes sooner for the step. This latter peak has mainly been assigned to the hybridization of O 2*p* states with Fe 4*sp* states[11] creating unoccupied states in the O 2*p* band. These differences in the shape of the B peak are entirely consistent with the differences in shape between the work of Saeterli *et* al.[9] for $BiFeO_3$ and $Bi_{0.9}La_{0.1}FeO_3$ and that of Paterson and Krivanek for Fe_2O_3.[10] No significant difference of the shape of the B peak was found in that latter work for the two different forms of Fe_2O_3 and therefore the A peak is more helpful in distinguishing these structural differences, as discussed above.

Within the Fe $L_{2,3}$ edge shown in Figure 3(j), no shoulder on the low energy side of the L_3 white line is observed, which occurs due to octahedral crystal field splitting, particularly for Fe^{3+},[12] including in rhombohedral $BiFeO_3$,[13] although not for more symmetric structures such as the supertetragonal T-phase.[13] Moreover, there is no detectable change in this ELNES between the perovskite and the step, which would suggest that the Fe is in the same 3+ oxidation state in the step as in the surrounding matrix. Moreover, it suggests that the ions in the step are very similarly octahedrally coordinated at the steps as in the perovskite matrix. Seeing as the surroundings of the antiphase boundaries are already known to exist in a structure rather similar to the T-phase,[4] it should be no surprise that Fe $L_{2,3}$ spectra, rather similar to these previous reports, are seen in this case. This suggests that the coordination of the Fe in the steps is either in tetragonally distorted or undistorted octahedra, rather than in rhombohedrally distorted octahedra.

A 3D structural model of the step was constructed using the atom positions determined from the HAADF and BF imaging, together with the assignment that all four B-sites are Fe, as confirmed by the EELS. However, due to the bending as the sample becomes thin, together with scanning distortions at the left-hand side of the boundary, averaged errors are up to 25 pm.

However, for the step, the second projection of ⟨001⟩ direction would give overlaps and consequently no clear atomic resolution images of steps would be possible from this orthogonal direction. Atom positions in the beam direction were therefore chosen on the assumption that these are the same as those determined for the equivalent positions in the terraces previously published.[4] This was considered a reasonable assumption since there is always a continuous boundary between the terraces and the steps. The resulting model is shown in Fig. 4. For the purposes of the model, it was assumed all the A-site atoms are Bi and all the B-site atoms are occupied with Fe though in reality

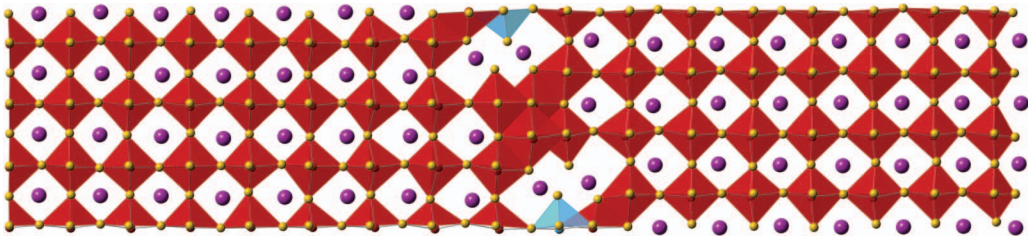

FIG. 4. A quantitative atomic model of the atomic structure of a step determined from the data presented in this work. Yellow atoms are O, purple atoms are Bi, red octahedra are FeO_6 octahedra, and the blue polyhedra at the edges are halves of TiO_6 octahedra at the start of the terrace to either side.

there should be some Nd and Ti distributed randomly. An xyz file giving a model of the structure is included as the supplementary material.[14]

The FeO_6 octahedra in this model of the step are now all edge sharing, consistent with the centres of the terraces. The unit cell origin is thus shifted by half the width of an octahedron in both directions, creating an antiphase relationship of cells on either side, similar to the planar antiphase boundaries reported previously.[4] This structure of 4 edge-sharing octahedra is also related to the structure of γ-Fe_2O_3, where all the octahedra share edges, and may well explain the ELNES results where the O-ELNES is similar to that for γ-Fe_2O_3. The Fe-ELNES suggests a 3+ oxidation state similar to the matrix with no discernible distortion of the octahedra, thereby preventing detectable splitting of the Fe-L_3 white line.

To verify the model, image simulation was carried out with a frozen phonon multislice approach using the QSTEM package[15] and an average of 30 phonon configurations in all calculations. Simulation conditions were chosen to correspond closely to the experiment (i.e., 100 kV electrons, 30 mrad convergence angle, no significant aberrations of the probe included, slices of half a primitive unit cell in thickness, i.e., 1.95 Å). A thickness of 40 primitive perovskite unit cells (∼15.4 nm) gave a reasonable qualitative match to the contrast. Magnified versions of HAADF and BF images of one step are shown in Figs. 2(a) and 2(b), above simulations of the same in Figs. 2(c) and 2(d). It is clear that all key features of the experimental images are reproduced in the simulations, even if there are some slight discrepancies in BF (probably arising from sample bending close to the edge, and damaged surfaces on the sample). Thus, it is clear that the model provides a reasonable match, giving confidence in the proposed 3D structure.

As with terraces previously studied,[4] there is an excess of negative charge at the steps, which compensates for the slight excess of positive charge in the matrix due to $Fe_{Ti}^{\bullet}$. Full occupancy of all sites in the step has been calculated to give a planar charge density of $-1.1\ C\,m^{-2}$. The charge density on the terraces was determined in our previous study to be a little lower at $-0.68\ C\,m^{-2}$;[4] the increased excess charge density at the steps will be due to the fact that Ti^{4+} is replaced by Fe^{3+} at these features. Such a high charge density would be expected to result in strong polarisation around the steps, which is indeed observed with noticeable movement of O columns away from the steps, Bi columns towards the steps, and large pseudotetragonal distortion of the cells to something analogous to the supertetragonal T-phase.[4,13,16]

Of course, one final feature of interest is why these stepped boundaries are formed. Clearly, the Ti-rich planar sections will have been formed by self-assembly during sintering in Ti-rich regions of the sample. Once an antiphase boundary has nucleated, then there is a half cell shift of the perovskite lattices to either side, and the boundary must either continue to grow or be terminated by a partial dislocation. This will mean that in general, the antiphase boundary must continue to grow laterally, even if locally, the titanium supply is insufficient to allow the continuation of the Ti-rich terrace. In this case, growing a step structure using the abundant Fe atoms will provide a viable alternative. Such stepped structures can clearly grow a fair distance if there is insufficient Ti locally to grow large terraces.

In summary, a novel stepped structure for antiphase boundaries in Ti-doped $BiFeO_3$ has been discovered, which is closely related to the novel planar antiphase boundaries discovered recently

in the same material. The atomic structure and chemistry of the steps were determined using a combination of HAADF and BF STEM imaging, and electron energy loss spectroscopy (including both elemental mapping and ELNES at both the O-K and Fe-$L_{2,3}$ edges). The core of each step consists of four columns of Fe atoms, each of which is octahedrally coordinated with the octahedra being arranged in an edge-sharing configuration. This model was tested by image simulations using the multislice frozen phonon approach and the simulations showed good qualitative agreement with the experimental images reproducing all principal features, and thus validating our proposed structure. As with the previously reported planar terraces on the antiphase boundaries, there appears to be more oxygen in the structure than required for charge neutrality, which would make the steps negatively charged. The negative charge at the steps has been estimated as $-1.1\ \mathrm{C\,m^{-2}}$. This has the result of inducing a local electric field, with the result that adjacent perovskite unit cells are visibly polarised with a vector normal to the boundary.

The authors gratefully acknowledge the support of the EPSRC for this work, including the provision of a Ph.D. studentship for LQW, support for the work on doping in bismuth ferrite at Sheffield (EP/G069069/1 and EP/G005001/1), and support for the work at SuperSTEM (EP/I000879/1, EP/J009679/1, and EP/J009628/1), as well as for the ongoing support for the SuperSTEM facility. We are also very thankful to Dr. Lothar Houben at the FZ-Jülich for the provision of the iMtools software used for the quantitative image analysis and to Professor Christoph Koch at the University of Ulm for advice and help with the STEM image simulations using QSTEM.

[1] K. Kalantari, I. Sterianou, S. Karimi, M. C. Ferrarelli, S. Miao, D. C. Sinclair, and I. M. Reaney, Adv. Funct. Mater. **21**, 3737 (2011).
[2] I. MacLaren, L. Q. Wang, B. Schaffer, Q. M. Ramasse, A. J. Craven, S. M. Selbach, N. A. Spaldin, S. Miao, K. Kalantari, and I. M. Reaney, Adv. Funct. Mater. **23**, 683 (2013).
[3] I. M. Reaney, I. MacLaren, L. Q. Wang, B. Schaffer, A. Craven, K. Kalantari, I. Sterianou, S. Karimi, and D. C. Sinclair, Appl. Phys. Lett. **100**, 182902 (2012).
[4] I. MacLaren, L. Q. Wang, O. Morris, A. J. Craven, R. L. Stamps, B. Schaffer, Q. M. Ramasse, S. Miao, K. Kalantari, I. Sterianou, and I. M. Reaney, APL Mater. **1**, 021102 (2013).
[5] I. MacLaren, R. Villaurrutia, B. Schaffer, L. Houben, and A. Pelaiz-Barranco, Adv. Funct. Mater. **22**, 261 (2012).
[6] R. Brydson, Mater. Sci. Tech. **16**, 1187 (2000).
[7] F. T. Docherty, A. J. Craven, D. W. McComb, and J. Skakle, Ultramicroscopy **86**, 273 (2001).
[8] T. J. Park, S. Sambasivan, D. A. Fischer, W. S. Yoon, J. A. Misewich, and S. S. Wong, J. Phys. Chem. C **112**, 10359 (2008).
[9] R. Saeterli, S. M. Selbach, P. Ravindran, T. Grande, and R. Holmestad, Phys. Rev. B **82**, 064102 (2010).
[10] J. H. Paterson and O. L. Krivanek, Ultramicroscopy **32**, 319 (1990).
[11] F. M. F. De Groot, M. Grioni, J. C. Fuggle, J. Ghijsen, G. A. Sawatzky, and H. Petersen, Phys. Rev. B **40**, 5715 (1989).
[12] K. M. Krishnan, Ultramicroscopy **32**, 309 (1990).
[13] M. D. Rossell, R. Erni, M. P. Prange, J. C. Idrobo, W. Luo, R. J. Zeches, S. T. Pantelides, and R. Ramesh, Phys. Rev. Lett. **108**, 047601 (2012).
[14] See supplementary material at http://dx.doi.org/10.1063/1.4884684 for an xyz file of the atomic structure of the step for viewing in crystallographic software packages.
[15] C. Koch, Ph.D. thesis, Arizona State University, 2002. The QSTEM package may be accessed and installed from http://elim.physik.uni-ulm.de/?page_id=834.
[16] R. J. Zeches, M. D. Rossell, J. X. Zhang, A. J. Hatt, Q. He, C. H. Yang, A. Kumar, C. H. Wang, A. Melville, C. Adamo, G. Sheng, Y. H. Chu, J. F. Ihlefeld, R. Erni, C. Ederer, V. Gopalan, L. Q. Chen, D. G. Schlom, N. A. Spaldin, L. W. Martin, and R. Ramesh, Science **326**, 977 (2009).